Elliptic flow and incomplete equilibration

J. L. Liu, Q. C. Feng, Q. S. Wang, G. X. Tang, J. B. Zhang, and L. Huo*
Department of Physics, Harbin Institute of Technology, Harbin 150001, People's Republic of China
(Received 25 December 2008; published 18 June 2009)

The dependence of eccentricity scaled elliptic flow on the partonic cross section in Au + Au collisions at relativistic heavy ion collider (RHIC) energy $\sqrt{s_{NN}} = 200$ GeV with impact parameter $b = 8$ fm is analyzed using a multiphase transport (AMPT) model. It is shown that the dependence of eccentricity scaled elliptic flow on the partonic cross section could be described well by a formula suggested by Bhalerao *et al.* The eccentricity scaled elliptic flow of the parton is 19% ∼ 27% lower than its 'hydrodynamic limit.' The hadronization of the parton through coalescence and hadronic dynamics (decay, collision) could influence the obtained deviation of eccentricity scaled elliptic flow of the hadron from its 'hydrodynamic limit.' The hadronic final state interactions and hadronization reduce the extracted 'hydrodynamic limit' by 20% and also reduce the deviation from the 'hydrodynamic limit' by 26%.

DOI: 10.1103/PhysRevC.79.064905 PACS number(s): 25.75.Ld, 25.75.Nq, 24.10.Jv

I. INTRODUCTION

The purpose of ultrarelativistic heavy ion collisions is to create nuclear matter under extremely high temperature and pressure conditions and study its properties. It is speculated that the quark and gluon plasma created at RHIC is strongly coupled [1–5]. The large elliptic flow value observed in the experiments [6–15] could be described by ideal relativistic hydrodynamics [16,17] and the transport model with an unphysically large cross section [18–26] (recently, a transport model including perturbative $3 \leftrightarrow 2$ interactions in gluon matter could explain most of the elliptic flow at RHIC [27,28]). Since the conditions, local equilibrium and/or nonviscous, are required by ideal relativistic hydrodynamics, the consistence between theoretical description and experimental data on elliptic flow at a small transverse momentum region ($p_T < 1.5$ GeV/c) and the dependence of differential elliptic flow on hadron species as a function of transverse momentum leads to the claim that the matter produced in RHIC experiments is the most "perfect fluid" [29]. However, this claim is still debatable [30–32]. The minimal ratio of shear viscosity to entropy has been calculated in Refs. [33,34]. The effects of viscosity on elliptic flow are studied in Refs. [27,28,35–40].

Elliptic flow results from the conversion of spatial anisotropy to momentum anisotropy in noncentral heavy ion collisions. It is sensitive to the properties of the system at the early stage because of its self-quenching character [3,41–43]. In the hydrodynamics scenario, the matter produced at the initial stage is assumed under local equilibrium, and the pressure gradient in the x direction (impact parameter direction) is larger than in the y direction (perpendicular to impact parameter direction and beam axis) in noncentral collisions. Therefore, larger transverse momentum of matter in the x direction than in the y direction is produced at the final state of collisions. Generally, elliptic flow is defined as the second order coefficient of the Fourier expansion of the particle azimuthal distribution with respect to the reaction plane [44,45]

$$E\frac{\mathrm{d}^3N}{\mathrm{d}^3p} = \frac{1}{2\pi}\frac{\mathrm{d}^2N}{p_T\mathrm{d}p_T\mathrm{d}y}\left(1+\sum_{n=1}^{\infty}2v_n\cos[n(\phi-\Psi_r)]\right), \quad (1)$$

where Ψ_r denotes the reaction plane angle (determined by the impact parameter direction and the beam axis) and it is zero in our calculations, and the sine terms vanish due to the reflection symmetry with respect to the reaction plane.

Recently, Bhalerao *et al.* suggested a formula which was expected to quantitatively describe the deviation of elliptic flow from the 'hydrodynamic limit' for gas under an incomplete equilibration condition [30,31]:

$$\frac{v_2}{\varepsilon} = \frac{v_2^{\mathrm{hydro}}}{\varepsilon}\frac{K^{-1}}{K^{-1}+K_0^{-1}}, \quad (2)$$

where ε is the eccentricity of the overlap region of the medium at initial time; v_2^{hydro} was interpreted as the hydrodynamic limit of elliptic flow; K_0 was assumed to be a constant and should be determined by fitting this formula to data; K was the Knudsen number, which is defined as

$$K^{-1} = \frac{\tilde{R}}{\lambda}, \quad (3)$$

where $\tilde{R} = 1/\sqrt{\frac{1}{\langle x^2\rangle}+\frac{1}{\langle y^2\rangle}}$ is the system size [30], and $\lambda = 1/\rho\sigma$ is the mean free path of the particle. Because of the strongly longitudinal expansion of the medium at RHIC energy, the particle density ρ decreases as the inverse of time τ [30]:

$$\rho = \frac{1}{\tau S}\frac{\mathrm{d}N}{\mathrm{d}y}, \quad (4)$$

where $\mathrm{d}N/\mathrm{d}y$ denotes the total multiplicity per unit rapidity, and $S = 4\pi\sqrt{\langle x^2\rangle\langle y^2\rangle}$ is the transverse overlap area between the two nuclei. It was argued in Ref. [30] that K should be estimated at the timescale, $\tau = \tilde{R}/c_s$, when elliptic flow is built up, i.e.,

$$\frac{1}{K} = \frac{\sigma}{S}\frac{\mathrm{d}N}{\mathrm{d}y}c_s, \quad (5)$$

*lhuo@hit.edu.cn

where c_s is the sound velocity of the fluid. The timescale $\tilde{R}/c_s$ was interpreted as the time when all parts of the system are "informed" about the initial spatial anisotropy (from the viewpoint of hydrodynamics), i.e., the buildup of elliptic flow. Recently, Eq. (2) was used to describe the elliptic flow of a two-dimensional massless gas [32] and was used to fit data [31].

In this paper, we study the dependence of elliptic flow on the partonic cross section using a multiphase transport model (AMPT) with impact parameter $b = 8$ fm. We use Eqs. (2) and (5) to fit the elliptic flow data from the model and extract the deviation from the 'hydrodynamic limit.' The paper is organized as follows. In Sec. II, a brief description of AMPT model is introduced. In Sec. III, the partonic elliptic flow with different partonic cross section is fitted with Eqs. (2) and (5). The deviation from the 'hydrodynamic limit' is extracted. In Sec. IV, the hadronic elliptic flow with different partonic cross section is fitted with Eqs. (2) and (5). The deviation from the 'hydrodynamic limit' is extracted. In Sec. VI, a brief summary is given.

II. AMPT MODEL

The AMPT model is a transport model [20] including both partonic and hadronic phase dynamics. Two different scenarios, i.e., default and string melting, are implemented in AMPT model. The string melting scenario has been used to reproduce RHIC elliptic flow [20–26] and HBT [20,46] data. In the string melting scenario, the initial partons are produced by converting the hadrons produced by using the HIJING model [47] to their valence quarks and antiquarks with current masses. The collisions between the produced partons are implemented by using the Zhang's parton cascade (ZPC) model [48]. Only the elastic collisions between partons are included in the ZPC model with the elastic differential cross section:

$$\frac{\mathrm{d}\sigma_0}{\mathrm{d}t} \approx \frac{9\pi\alpha_s^2}{2}\left(1+\frac{\mu^2}{s}\right)\frac{1}{(t-\mu^2)^2}, \tag{6}$$

and the total cross section is

$$\sigma_0 \approx \frac{9\pi\alpha_s^2}{2\mu^2}, \tag{7}$$

where the strong coupling constant α_s is 0.4714; s and t are Mandelstam variables; μ is the screen mass and could be adjusted to fix total cross section. The total cross section is 3 mb in the pQCD calculation, but a large cross section 6–10 mb has to be used to describe RHIC elliptic flow data. After stopping interactions (freeze-out), the two nearest quarks and antiquarks in spatial space are combined to form a meson and the three nearest quarks or antiquarks in spatial space are combined to form a baryon or antibaryon. Interactions between hadrons are implemented by using a relativistic transport (ART) model [49]. The incomplete equilibration has been included in AMPT model dynamically. In this paper, we simulate Au + Au collisions at RHIC energy $\sqrt{s_{NN}} = 200$ GeV with impact parameter $b = 8$ fm for different partonic cross sections as we did in Ref. [50]. The version of AMPT model used in this paper is v2.11, and 10 000 events are produced for each cross section. The random seed is the obtained runtime. In the following sections, our calculations focus on the midrapidity region ($-1 < y < 1$).

III. PARTONIC ELLIPTIC FLOW

Strictly speaking, Eqs. (2) and (5) was obtained assuming the sound velocity c_s is constant and the number of particles is conserved (elastic collision) during the evolution of the medium, and it was only tested for 2D massless gas under these two conditions with an isotropic cross section and Gaussian distribution of the particle in the transverse plane [32]. In AMPT model, although hadron dynamics does not conserve the number of hadrons, the parton cascade conserves the number of partons. Furthermore, the masses of partons are their current masses, so the parton could be considered as a massless particle. We also have checked that the distribution of the parton at initial time is approximately Gaussian. Thus, we expect Eq. (2) could be used to describe the elliptic flow data from AMPT model, at least for partons.

As shown in Eq. (5), the elliptic flow of the partons in Eq. (2) could be plotted as a function of $\frac{\mathrm{d}N}{S\mathrm{d}y}$ or σ or their product. In Ref. [31] Eq. (1) was used to fit the data as a function of $\frac{\mathrm{d}N}{S\mathrm{d}y}$. However, in order to obtain good agreement with the data, the eccentricity fluctuation of the participant nucleons should be carefully considered. Based on the model data we analyzed in Ref. [50], we will plot Eq. (1) as a function of $\frac{\sigma}{S}\frac{\mathrm{d}N}{\mathrm{d}y}c_s$ ($\frac{\mathrm{d}N}{S\mathrm{d}y}$ is almost independent of partonic cross section and c_s, in fact, is a constant). For collisions with fixed impact parameter, the eccentricity fluctuation of the participant nucleons should be expected to be not important for our results for different cross sections, except for a scale factor for elliptic flow.

One should note some important differences between the AMPT model and the model constructed in Ref. [32]. In AMPT model, the partons could move in three-dimensional spatial space, but only 2D transverse moving is allowed in the model used in Ref. [32]. It was argued in Ref. [32] that the same result should be obtained for a 3D massless gas as 2D case assuming the validity of the longitudinal boost invariant. However, this expectation has still not been tested exactly. Another difference is the differential cross section which is isotropic in the model used in Ref. [32] but is a Debye screened one in AMPT model for partons. As discussed in Ref. [32], one should use the isotropic cross section in Eq. (2) and the Debye screened one should be converted to the isotropic one. For the production of elliptic flow, the transport cross section should be the relevant one, i.e., the elliptic flow only depends on the transport cross section if other conditions are fixed ($\mathrm{d}N/S\mathrm{d}y, T, b$) [19]. For the differential cross section used in Eq. (6), the transport cross section could be expressed as [19]

$$\begin{aligned}\sigma_t &\equiv \int \mathrm{d}\sigma_{el}\sin^2\theta_{\mathrm{c.m.}} \\ &= \int \mathrm{d}t\frac{\mathrm{d}\sigma_{el}}{\mathrm{d}t}\frac{4t}{s}\left(1-\frac{t}{s}\right) \\ &= \sigma_0 4z(1+z)\left[(2z+1)\ln(1+1/z)-2\right],\end{aligned} \tag{8}$$

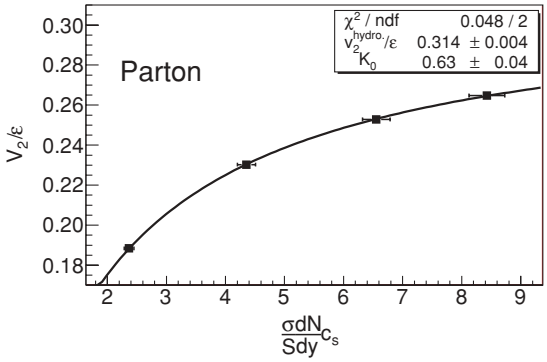

FIG. 1. Elliptic flow of the parton for different partonic cross sections. The solid line is the fitting result of Eqs. (2) and (5) to data from AMPT model (see text).

where $z \equiv \mu^2/s$. For the isotropic case ($\mu \to \infty$), $\sigma_t/\sigma_0 = 2/3$. Thus, for the differential cross section in Eq. (6), the equivalent isotropic cross section is

$$\sigma = \frac{3\sigma_0}{2}\frac{\sigma_t}{\sigma_0}. \tag{9}$$

To the calculations for partons in present paper, the average c.m.s. energy is $s \approx 0.35\,\mathrm{GeV}^2$ and $s \approx 0.21\,\mathrm{GeV}^2$ for partons at initial time and final time ($t \to \infty$), respectively. s is calculated for parton pairs in midrapidity in AMPT model directly. Since the elliptic flow is mainly built up at the early time of the evolution of the system, we set $s \approx 0.35\ \mathrm{GeV}^2$ as our default choice. In AMPT model, the total elastic cross section σ_0 in Eq. (7) is fixed by tuning μ, so the ratio of σ_t to σ_0 varies for different cross sections.

In Fig. 1 we plot the eccentricity scaled elliptic flow of the parton v_2/ε as a function of $\frac{\sigma}{S}\frac{dN}{dy}c_s$ for Au + Au collisions at $\sqrt{s_{NN}} = 200$ GeV with fixed impact parameter $b = 8$ fm and $\sigma_0 = 3,\ 6,\ 10,\ 14$ mb. Table I gathers relevant parameters for the parton. The horizontal error bar in Fig. 1 is due to the statistical fluctuation of the partons' multiplicity ($\sim \sqrt{N}$) and the vertical error bar (too small to be seen) denotes the error obtained when we use Eq. (1) to fit the partons' azimuthal distribution. The sound velocity c_s of the massless gas is used, i.e., $c_s = 1/\sqrt{3}$. The isotropic cross section is obtained through Eq. (9). The transverse area S is calculated for partons at initial time as done in Ref. [32]. The eccentricity is calculated for partons at initial time as

$$\varepsilon = \frac{\langle y^2\rangle - \langle x^2\rangle}{\langle y^2\rangle + \langle x^2\rangle}, \tag{10}$$

where the bracket denotes the average over partons and events. In Ref. [32], dN/dy is in fact independent of time because only 2D gas is considered, but dN/dy varies with time slightly in AMPT model. In plotting Fig. 1, dN/dy of partons at the final time is used. The solid line is the best fit of Eq. (2) to the model data, with fitted parameters $v_2^{\mathrm{hydro}}/\varepsilon \approx 0.314 \pm 0.004$ and $K_0 \approx 0.63 \pm 0.04$. Given the 'hydrodynamic limit' $v_2^{\mathrm{hydro}}/\varepsilon$, we could give a quantitative description of the deviation of v_2/ε from its limiting value, which is 27% and 19% lower than $v_2^{\mathrm{hydro}}/\varepsilon$ for $\sigma_0 = 6$ mb and 10 mb, respectively. This deviation indicates that the local equilibration of the system is still not achieved and the elliptic flow could be increased much more for the conditions considered in this paper. The incomplete equilibration of the system in AMPT model was studied in a recent paper [52]. Both the cross section $\sigma_0 = 6$ mb and 10 mb in AMPT model could reproduce the elliptic flow data, but $\sigma_0 = 10$ mb could reproduce the high-order anisotropy flow data [53].

TABLE I. Parameters for the parton. See text for details.

σ_0(mb)	ε	S(fm^2)	$\frac{dN}{dy}$(initial)	$\frac{dN}{dy}$(final)
3	0.2835	57.76	885.4	815.6
6	0.2861	57.77	886.5	797.9
10	0.2833	57.85	886.5	782.5
14	0.2831	57.83	887.4	773.1

In Ref. [32], $Ry = 1.5\,Rx$ corresponding to $\varepsilon \approx 0.38$ and $v_2^{\mathrm{hydro}} \approx 0.10$ result in $v_2^{\mathrm{hydro}}/\varepsilon \approx 0.26$. However, in Ref. [51], $v_2^{\mathrm{hydro}}/\varepsilon \approx 0.36$ is expected for the hydrodynamics model for the 3D massless gas equation. Detailed calculations would be needed in order to compare these 'hydrodynamic limit' values, especially concerning the difference of the initial conditions, which is not the scope of this paper. In the present paper we just consider the fitted $v_2^{\mathrm{hydro}}/\varepsilon$ as the limit of v_2/ε when the partonic cross section is enlarged. This is the reason we use the quoted word 'hydrodynamic limit.' If we replace dN/dy in Fig. 1 with its value for partons at initial time, we get the fitted parameters $v_2^{\mathrm{hydro}}/\varepsilon \approx 0.309 \pm 0.004$ and $K_0 \approx 0.60 \pm 0.04$, which is little change relative to the value obtained above. In the following, our calculations will be done with dN/dy for partons at final time.

The parameter K_0 obtained is 0.63 ± 0.04. Considering the error of K_0, it is consistent with the suggested value $K_0 \approx 0.70 \pm 0.03$ obtained in Ref. [32]. However, K_0 is sensitive to the conditions one set, for example, if we set the c.m.s. energy as $s \approx 0.21\,\mathrm{GeV}^2$ instead of $0.35\,\mathrm{GeV}^2$, then: (1) $K_0 \approx 0.65 \pm 0.04$ and $v_2^{\mathrm{hydro}}/\varepsilon \approx 0.307 \pm 0.003$, if dN/dy of the partons at final time is used; (2) $K_0 \approx 0.62 \pm 0.03$ and $v_2^{\mathrm{hydro}}/\varepsilon \approx 0.304 \pm 0.003$, if dN/dy of the partons at initial time is used. The error of K_0 is sensitive to the error of the data from the model. In plotting Fig. 1, we only take into account the errors of $\frac{dN}{dy}$ and v_2. The errors of other variables in Eqs. (2) and (5) would enlarge the error of K_0. In Ref. [32], the authors found that K_0 was sensitive to the diluteness of gas. From the results of Ref. [32] one could find that the value of K_0 would be smaller than 0.7 if the gas is not dilute enough. Right now, we do not know whether this is the whole reason that our value K_0 is a little smaller than 0.7, because the value 0.7 is only a suggested value for 3D case gas but not proved in Ref. [32] and K_0 is sensitive to some conditions discussed above. However, Eqs. (2) and (5) seem to be robust enough to be applied even if the gas is not dilute enough as shown in Ref. [32].

In conclusion, Eqs. (2) and (5) fit the AMPT model data of partons for Au + Au collisions at $\sqrt{s_{NN}} = 200$ GeV with an impact parameter $b = 8$ fm and different partonic cross sections well. The obtained parameters are $v_2^{\mathrm{hydro}}/\varepsilon \approx 0.314 \pm 0.004$ and $K_0 \approx 0.63 \pm 0.04$. The deviation of the eccentricity

TABLE II. Parameters for the hadron. See text for details.

σ_0(mb)	ε(h.h.)	S(h.h.)(fm^2)	$\frac{dN}{dy}$(h.h.)	$\frac{dN}{dy}(c)$	$\frac{dN}{dy}(f)$
3	0.2855	57.54	424.3	427.4	587.6
6	0.2880	57.55	425.0	424.9	575.0
10	0.2851	57.63	424.8	420.3	565.7
14	0.2847	57.63	425.2	416.8	560.6

scaled elliptic flow v_2/ε for the cross section $\sigma = 6$ and 10 mb is 27% and 19% below its 'hydrodynamic limit.' Given the parameters $v_2^{\rm hydro}/\varepsilon$ and K_0, Eqs. (2) and (5) could be used to predict the eccentricity scaled elliptic flow with other cross section values.

IV. HADRONIC ELLIPTIC FLOW

As we mentioned in the above section, Eqs. (2) and (5) is obtained for a system in which the sound velocity c_s is constant and the number of the particle is conserved [30] and is tested only for a 2D massless gas [32]. For the system of 3D hadrons, these requirements are not guaranteed generally. Interestingly, Eqs. (2) and (5) could give a good description to the experimental data [31]. In this section we assume the validity of Eqs. (2) and (5) as Ref. [31] and fit Eq. (2) to the elliptic flow data of the hadron from AMPT model.

We analyze the elliptic flow of the hadron at two different stages: the hadron at the final time, for which the relevant variables will be marked by 'f' and the hadron just after partons are coalesced (see Sec. II), for which the relevant variables will be marked by 'c.' For consistency, the initial condition (S, ε) is determined from the hadrons after HIJING is finished (see Sec. II). Table II gathers relevant parameters for the hadron, "h.h." denotes hadrons from HIJING. Using the initial condition of partons at initial time would almost not change the results, the difference is $< 2\%$.

In Fig. 2 we plot the eccentricity scaled elliptic flow of hadron(c) $v_2(c)/\varepsilon$ as a function of $\frac{\sigma}{S}\frac{dN(c)}{dy}c_s$ for the same conditions as in Sec. II. So far, we do not know how to give a good description of the cross section and sound velocity c_s for a dynamic model including the hadron. However, since the elliptic flow is mainly produced at the partonic stage [54], we use the value of c_s and σ in parton stage for $\frac{\sigma}{S}\frac{dN(c)}{dy}c_s$ in Fig. 2. The fitted parameters $v_2^{\rm hydro}(c)/\varepsilon \approx 0.317 \pm 0.003$ and $K_0(c) \approx 2.4 \pm 0.2$. For the simple quark coalescence model, the differential elliptic flow of the hadron at intermediate transverse momentum is 2 or 3 times the elliptic flow of the parton. However, for the realistic condition and dynamic model [23,55,56], the simple quark number scaling could not be expected generally. The case may become even worse if one considers the integral elliptic flow, because the binding energy and unitary problems would be important [56,57]. Thus, we could not expect any simple scale for the elliptic flow of the hadron relative to that of the parton. The larger value of $K_0(c)$ in Fig. 2 than that in Fig. 1 is partially due to the difference of dN/dy for the parton and hadron. If we convert the hadrons produced through coalescence to their constituent quark, the ratio of the number of the parton to that of the hadron is approximately 2.2.

The deviation of the eccentricity scaled elliptic flow of hadron(c) $v_2(c)/\varepsilon$ from its 'hydrodynamic limit' for the cross section $\sigma = 6$ and 10 mb is 15% and 11%, respectively. These values are smaller than the values obtained for partons. We find that the ratio of elliptic flow of hadron(c) to that of the parton varies from $1.27 \sim 1.1$ for the cross section $3 \sim 14$ mb. This result leads to two effects on the elliptic flow of hadron(c): (1) the elliptic flow of hadron(c) is larger than that of the parton, which would increase $v_2(c)/\varepsilon$ and $v_2^{\rm hydro}(c)/\varepsilon$ relative to that of the parton; (2) the ratio of elliptic flow of hadron(c) to that of the parton is larger for smaller cross sections than larger ones, which would make the increasing of the elliptic flow of hadron(c) with the cross section less and reduce $v_2^{\rm hydro}(c)/\varepsilon$. The second effect reduces the deviation of the elliptic flow of hadron(c) from its 'hydrodynamic limit.' The combination of the above effects leads to the almost negligible effect of hadronization on $v_2^{\rm hydro}/\varepsilon$. We have checked that if we replace the value of elliptic flow of the hadron in Fig. 2 with the corresponding value of the parton, all the results are almost the same as the parton case in Sec. III, except for $K_0(c)$. If we consider the factor 2.2 (ratio of number of partons to that of hadrons) mentioned above, the fitted K_0 is almost the same for both cases. This result indicates that when Eqs. (2) and (5) are used to fit experimental data, one should take care of

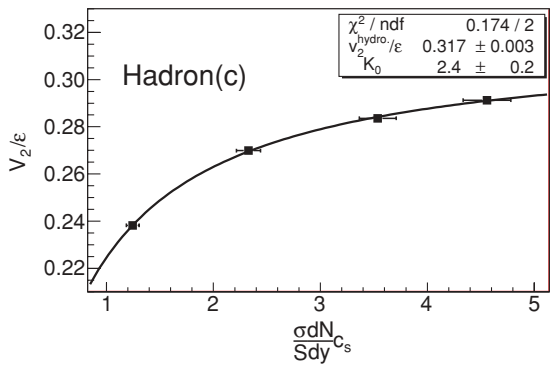

FIG. 2. Elliptic flow of the hadron(c). The solid line is the fitting result of Eqs. (2) and (5) to data from AMPT model (see text).

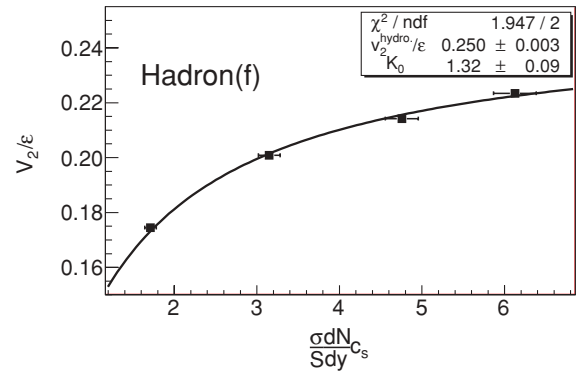

FIG. 3. Elliptic flow of the final hadron for different partonic cross sections. The solid line is the fitting result of Eqs. (2) and (5) to data from AMPT model (see text).

the interpretation of the variables in Eq. (5). For example, if one would interpret the cross section in Eq. (5) as a partonic cross section one may have to divide the fitted cross section by $2 \sim 3$.

In Fig. 3 we plot the eccentricity scaled elliptic flow of hadron(f) $v_2(f)/\varepsilon$ as a function of $\frac{\sigma}{S}\frac{dN(f)}{dy}c_s$ with the same conditions as in Sec. III. The fitted parameters $v_2^{\rm hydro}(f)/\varepsilon \approx 0.250 \pm 0.003$ and $K_0(f) \approx 1.32 \pm 0.09$. The smaller value of the elliptic flow of hadron(f) than that of hadron(c) may be due to the resonance decay process which would randomize the direction of the hadron. The deviation of $v_2(f)/\varepsilon$ from its 'hydrodynamic limit' for cross sections $\sigma = 6$ and 10 mb is 20% and 14%, respectively. Hadronic dynamics (decay, collisions) could modify both $dN(f)/dy$ and $v_2(f)/\varepsilon$ relative their value for hadron(c). If we replace $v_2(f)$ with $v_2(c)$ but keep $dN(f)/dy$ unchanged, the deviation from the 'hydrodynamic limit' is almost the same as for the case of hadron(c); if we replace $dN(f)/dy$ with $dN(c)/dy$ but keep the elliptic flow unchanged, the deviation from the 'hydrodynamic limit' is almost unchanged. $K_0(f)$ is sensitive to both the $v_2(f)$ and $dN(f)/dy$.

In conclusion, Eqs. (2) and (5) fits the AMPT model data of the hadron in Au + Au collisions at $\sqrt{s_{NN}} = 200$ GeV with an impact parameter $b = 8$ fm and different partonic cross sections well. The deviation of the eccentricity scaled elliptic flow v_2/ε from its 'hydrodynamic limit' for cross sections $\sigma = 6$ and 10 mb is influenced by the coalescence process and hadronic dynamics. The hadronic final state interactions and hadronization reduce the extracted 'hydrodynamic limit' by 20% and also reduce the deviation from the 'hydrodynamic limit' by 26%. One could expect that the influence of the coalescence process and hadronic dynamics would also appear when Eqs. (2) and (5) are used to describe the experimental data.

V. SUMMARY

We analyze the dependence of eccentricity scaled elliptic flow on the partonic cross section in Au + Au collisions at RHIC energy $\sqrt{s_{NN}} = 200$ GeV with an impact parameter $b = 8$ fm using AMPT model. It is shown that the dependence of eccentricity scaled elliptic flow on the partonic cross section could be described well by a formula suggested by Bhalerao *et al.* The eccentricity scaled elliptic flow of partons is 19% and 27% lower than its 'hydrodynamic limit' for cross sections $\sigma = 10$ and 6 mb, respectively. The deviation of eccentricity scaled elliptic flow of the hadrons from their 'hydrodynamic limit' could be influenced by both the hadronization of partons through coalescence and hadronic dynamics. The hadronic final state interactions and hadronization reduce the extracted 'hydrodynamic limit' by 20% and also reduce the deviation from the 'hydrodynamic limit' by 26%.

ACKNOWLEDGMENTS

This work is supported by the Science Foundation of Harbin Institute of Technology (HIT.2002.47, HIT.2003.33)

[1] T. D. Lee, Nucl. Phys. **A750**, 1 (2005).
[2] M. Gyulassy and L. McLerran, Nucl. Phys. **A750**, 30 (2005).
[3] E. V. Shuryak, Nucl. Phys. **A750**, 64 (2005).
[4] B. Muller, Nucl. Phys. **A750**, 84 (2005).
[5] H. Stocker, Nucl. Phys. **A750**, 121 (2005).
[6] S. S. Adler *et al.* (PHENIX Collaboration), Phys. Rev. Lett. **91**, 182301 (2003).
[7] J. Adams *et al.* (STAR Collaboration), Phys. Rev. Lett. **92**, 052302 (2004).
[8] J. Adams *et al.* (STAR Collaboration), Phys. Rev. C **72**, 014904 (2005).
[9] R. Nouicer (PHOBOS Collaboration), J. Phys. G: Nucl. Part. Phys. **34**, S887 (2007).
[10] P. Sorensen (STAR Collaboration), J. Phys. G: Nucl. Part. Phys. **34**, S897 (2007).
[11] A. Taranenko (PHENIX Collaboration), J. Phys. G: Nucl. Part. Phys. **34**, S1069 (2007).
[12] A. Adare (PHENIX Collaboration), Phys. Rev. Lett. **98**, 162301 (2007).
[13] S. Afanasiev (PHENIX Collaboration), Phys. Rev. Lett. **99**, 052301 (2007).
[14] B. I. Abelev (STAR Collaboration), Phys. Rev. Lett. **99**, 112301 (2007).
[15] B. I. Abelev (STAR Collaboration), Phys. Rev. C **75**, 054906 (2007).
[16] P. Houvinen, P. F. Kolb, U. Heinz, P. V. Ruuskanen, and S. A. Voloshin, Phys. Lett. **B503**, 58 (2001).
[17] P. F. Kolb and U. Heinz, in *Quark-Gluon Plasma 3*, edited by R. C. Hwa and X.-N. Wang (World Scientific, Singapore, 2004), see also references therein.
[18] B. Zhang, M. Gyulassy, and C. M. Ko, Phys. Lett. **B455**, 45 (1999).
[19] D. Molnar and M. Gyulassy, Nucl. Phys. **A697**, 495 (2002); **A703**, 893(E) (2002).
[20] Z. W. Lin, C. M. Ko, B. A. Li, B. Zhang, and S. Pal, Phys. Rev. C **72**, 064901 (2005), see also references therein.
[21] B. Zhang, L. W. Chen, and C. M. Ko, Phys. Rev. C **72**, 024906 (2005).
[22] L. W. Chen, V. Greco, C. M. Ko, and P. F. Kolb, Phys. Lett. **B605**, 95 (2005).
[23] L. W. Chen and C. M. Ko, Phys. Rev. C **73**, 044903 (2006).
[24] L. W. Chen and C. M. Ko, Phys. Lett. **B634**, 205 (2006).
[25] J. H. Chen *et al.*, Phys. Rev. C **74**, 064902 (2006).
[26] Meiling Yu, Jiaxin Du, and Lianshou Liu, Phys. Rev. C **74**, 044906 (2006).
[27] Z. Xu, C. Greiner, and H. Stocker, Phys. Rev. Lett. **101**, 082302 (2008).
[28] Z. Xu and C. Greiner, Phys. Rev. C **79**, 014904 (2009), see also references therein.
[29] M. J. Tannenbaum, Rep. Prog. Phys. **69**, 2005 (2006).
[30] R. S. Bhalerao, J. P. Blaizot, N. Borghini, and J. Y. Ollitrault, Phys. Lett. **B627**, 49 (2005).
[31] H. J. Drescher, A. Dumitru, C. Gombeaud, and J. Y. Ollitrault, Phys. Rev. C **76**, 024905 (2007).

[32] C. Gombeaud and J. Y. Ollitrault, Phys. Rev. C **77**, 054904 (2008).
[33] P. Kovtun, D. T. Son, and A. O. Starinets, Phys. Rev. Lett. **94**, 111601 (2005).
[34] M. Brigante *et al.*, Phys. Rev. Lett. **100**, 191601 (2008).
[35] D. Teaney, Phys. Rev. C **68**, 034913 (2003).
[36] D. Molnar and P. Huovinen, Phys. Rev. Lett. **94**, 012302 (2005).
[37] T. Hirano and M. Gyulassy, Nucl. Phys. **A769**, 71 (2006).
[38] P. Romatschke and U. Romatschke, Phys. Rev. Lett. **99**, 172301 (2007).
[39] H. C. Song and U. Heinz, Phys. Rev. C **77**, 064901 (2008).
[40] A. K. Chaudhuri, arXiv:0801.3180.
[41] J. Y. Ollitrault, Phys. Rev. D **46**, 229 (1992).
[42] H. Sorge, Phys. Rev. Lett. **82**, 2048 (1999).
[43] N. Xu, Nucl. Phys. **A751**, 109c (2005).
[44] S. Voloshin and Y. Zhang, Z. Phys. C **70**, 665 (1996).
[45] A. M. Poskanzer and S. A. Voloshin, Phys. Rev. C **58**, 1671 (1998).
[46] Z. W. Lin, C. M. Ko, and S. Pal, Phys. Rev. Lett. **89**, 152301 (2002).
[47] M. Gyulassy and X. N. Wang, Comput. Phys. Commun. **83**, 307 (1994).
[48] B. Zhang, Comput. Phys. Commun. **109**, 193 (1998).
[49] B. A. Li and C. M. Ko, Phys. Rev. C **52**, 2037 (1995).
[50] J. L. Liu, J. B. Zhang, G. X. Tang, and L. Huo, Phys. Rev. C **78**, 034911 (2008).
[51] M. Issah and A. Taranenko (PHENIX Collaboration), arXiv:nucl-ex/0604011.
[52] B. Zhang, L. W. Chen, and C. M. Ko, J. Phys. G: Nucl. Part. Phys. **35**, 065103 (2008).
[53] L. W. Chen, C. M. Ko, and Z. W. Lin, Phys. Rev. C **69**, 031901(R) (2004).
[54] Z. W. Lin and C. M. Ko, Phys. Rev. C **65**, 034904 (2002).
[55] D. Molnar, arXiv:nucl-th/0408044.
[56] S. Pratt and S. Pal, Phys. Rev. C **71**, 014905 (2005).
[57] D. Molnar and S. A. Voloshin, Phys. Rev. Lett. **91**, 092301 (2003).